J Therm Spray Tech (2020) 29:657–669
https://doi.org/10.1007/s11666-020-01001-0

PEER REVIEWED

Peening Effect of Glass Beads in the Cold Spray Deposition of Polymeric Powders

Zahra Khalkhali[1] · Kashyap Sundara Rajan[1] · Jonathan P. Rothstein[1]

Submitted: 31 July 2019 / in revised form: 5 February 2020 / Published online: 27 February 2020

Abstract Cold spray is a green additive manufacturing method that accelerates micron-size particles to supersonic speeds. At these high speeds, the particles deposit upon impact with a desired surface. High-density polyethylene, polyurethane, polyamide-12, polystyrene, and ultra-high molecular weight polyethylene particles were cold-sprayed onto a low-density polyethylene substrate under different process conditions. Glass beads with diameters between 20 and 120 μm were added to each batch to study the effect of non-adhesive peening particles on the deposition efficiency and the quality of the final deposited layer of a series different polymeric powders. The successful deposition window was compared for the cold spray process with and without the addition of glass beads. Adding the glass beads to the polymer powders was found to widen the successful windows of deposition to both higher and lower impact velocities at a given temperature for all the polymer powder studied. In addition, adding peening particles were found to make deposition possible at lower particle temperatures where deposition had not been successful previously. This was especially important for ultra-high molecular weight polyethylene particles for which deposition in the absence of peening particles was not possible below 60 °C, but with peening particles was successful even at room temperature. Peening particles were found to increase deposition efficiency by as much as 50% for a given set of deposition conditions. The appropriate size of the added glass beads to maximize the deposition efficiency was found to be comparable to the size of the depositing particles. The addition of glass beads was also found to reduce the surface roughness of the deposited layer by more than 50%. Finally, for processing conditions with particle velocities below a Mach number of one, no glass beads were found to adhere to the resulting cold-sprayed substrates.

Keywords additive glass beads · cold spray · peening · UHMWPE · window of deposition

Introduction

Over the last forty years, there has been extensive research on the cold spray process as a green additive manufacturing technique capable of depositing a variety of powder particles including metals, polymers, composites, and ceramics on various substrates (Ref 1, 2). In the cold spray deposition process, a preheated, high-pressure gas flows through a converging–diverging nozzle to form a supersonic jet. The feedstock particles are introduced into the supersonic gas flow and accelerated to high velocities before impacting the substrate surface. Upon impact, the dissipation of the particle's kinetic energy results in severe plastic deformation leading to strong chemical, metallurgical, and/or mechanical bonding at the particle/substrate interface (Ref 3-8). In the cold spray process, sprayed particles remain in their solid state during the entire deposition process minimizing chances of oxidation, degradation, residual stresses, and any other defects associated with high-temperature coating processes (Ref 7, 8). Microstructural or expansion mismatches are also prevented in this technique (Ref 3, 4). As no solvent is used in this method, cold spray is considered as a green additive manufacturing process. Cold spray has emerged as an

✉ Zahra Khalkhali
khalkhali_z@yahoo.com

[1] Department of Mechanical and Industrial Engineering, University of Massachusetts, Amherst, MA 01003, USA

important new coating technology with a number of applications in areas including biomaterials (Ref 9-11), photocatalysts (Ref 12), copper-based catalysts (Ref 13), antifouling surfaces (Ref 14, 15), antibacterial coatings (Ref 16), renewable energy (Ref 17), and the aerospace industry (Ref 5, 6, 16, 18-24).

In our previous work, a series of high glass transition temperature polystyrene (PS) and polyamide-12 (PA) powders were deposited on PS, PA, and low-density polyethylene (LDPE) substrates using both the cold spray technique and a single particle impact technique that used laser ablation to accelerate a single particle well beyond the speed of sound and observe as it impacts a solid substrate (Ref 4). The single particle impact studies provided information about the particle impact dynamics that could not be monitored during cold spray due to the sheer number of particles. These data included the plastic deformation of a successfully deposited particles and the coefficient of restitution of a rebounding particle during an unsuccessful deposition. Both PA and PS were found to deposit on the soft LDPE substrate at similar impact velocities using both deposition techniques. However, a number of differences between the two techniques were observed. The first major difference was that like-on-like deposition onto a substrate melt-cast from PA or PS particles was only found to be successful in cold spray. Like-on-like deposition was never successful for single particle impacts even at impact velocities of more than 400 m/s. The second major difference between the two techniques was that single particle impacts successfully deposited on LDPE with a deposition efficiency of essentially 100%, while, for the cold spray processes, the deposition efficiency was less than 5%. These results suggest multiple particle impacts and/or surface roughness can play a major role in the effectiveness and efficiency of the cold spray deposition process for polymers. In single particle impacts, the effect of successive particle collisions on the first deposited particle is eliminated. The enhanced plastic deformation in both the primary particle and the substrate beneath the primary particle due to the successive head-on particle collisions might explain why like-on-like deposition was achieved in the cold spray process but not in the single particle impact experiments. This observation suggests that the addition of some sacrificial, dense, non-adhesive particles like glass beads to the polymer particle batch could have a beneficial effect on deposition efficiency of polymeric cold spray. Our hypothesis is that these glass particles could be used to peen the surface thereby flattening weakly adhered particles, inducing an increased plastic deformation and mixing between the substrate and the polymer particles, and leaving the surface less rough for incoming polymer particles thereby increasing deposition efficiency. The objective of the present study is thus to investigate the effects of adding different amounts and sizes of glass beads to a series of polymer powders on the deposition window, the deposition efficiency, and the quality of the cold-sprayed coating.

Shot peening is a mechanical treatment to improve surface properties of materials by bombarding the surface with high-quality spherical media like steel, ceramic, or glass in a controlled operation. There are various types of shot peening including laser peening (Ref 25), wet shot peening (Ref 26), ultrasonic peening (Ref 27), and micro-shot peening (Ref 27). All these techniques result in the incorporation of residual compressive stresses into the surface, grain refinement and grain size reduction. In metals, shot peening is known to improve corrosion resistance and electrochemical properties (Ref 28) while also increasing its fatigue life (Ref 25, 26). Shot peening has applications in the treatment of ceramics and composites as well (Ref 29, 30) although it is not frequently used to treat polymer surfaces or coatings.

In recent years, shot peening has been studied before (Ref 31), during (Ref 32), and after (Ref 31) the cold spray process for some metals. For instance, in metallic cold spray, the shot peening process can eliminate the porosity (Ref 32), enhance the work hardening of the coating (Ref 33), or improve the fatigue performance of the cold-sprayed material (Ref 31). Luo et al. (Ref 32) added up to 70% large-sized stainless steel particles to the particle batch of pure metal and some alloys of titanium in a cold spray process and found that the peening effect from the steel shots decreased the porosity from 15 to 0.7% and increased the microhardness by 70%. However, about 3 vol.% of the steel particles was found to incorporate into the cold-sprayed coating. They also reported a slightly lower deposition efficiency after adding the 70% steel particles to the titanium pure metal and alloy. Moridi et al. (Ref 31) found shot peening of cold-sprayed specimens to be more effective when applied prior to the cold spray process. They increased the fatigue strength of aluminum by 26% with shot peening the aluminum substrate prior to cold spraying aluminum particles on it.

Although the addition of peening particles has not been used in the cold spray processing of polymeric powders, small metal particle have been added to polymeric powders in the past to improve the surface activity of the cold-sprayed polymeric particles to reinforce the bond between the particle and substrate (Ref 34). Ravi et al. (Ref 34) studied the cold spray deposition of 45–63 μm UHMWPE particles on aluminum. They found no deposition for gas temperature between 190 and 500 °C and particle impact velocity ranging between 170 and 220 m/s. Deposition was finally achieved, albeit with low efficiencies of DE= 1.4%, only after adding 10 wt.% of fumed alumina nanoparticles to the UHMWPE powders. They argued that the improved

adhesion was due to the hydrogen bonds created between the fumed alumina nanoparticles and the oxide layer on the aluminum surface. In their work, these particles do not peen the surface. They are too small and light. In our previous work (Ref 35), UHMWPE powders were deposited in the absence of nanoparticles at temperatures above T_p = 80 °C and velocities above 275 m/s, but, even though the deposition efficiency was found to be two orders of magnitude larger than Ravi et al. (Ref 34), it was still rather low at DE = 2.9%, and the window of deposition was quite narrow and limiting.

In the present study, glass beads of different sizes were added over a range of concentrations to polymer powders of high-density polyethylene (HDPE), polyurethane (PU), polyamide 12 (PA), polystyrene (PS), and ultra-high molecular weight polyethylene (UHMWPE). These mixtures were then studied using the cold spray deposition technique in order to understand the effect of the glass peening particles on the deposition efficiency, the deposition window, the surface roughness, and the final microstructure of the deposited layer.

Materials and Methods

In Table 1, the typical materials properties from the literature and the manufacturer are provided for the polymer particles studied here. These powder particles included: high-density polyethylene (HDPE), polyurethane (PU), polyamide-12 (PA), polystyrene (PS), and ultra-high molecular weight polyethylene (UHMWPE). These polymers have varied molecular architecture which leads to a range in modulus and glass transition temperature. All the particles used were roughly the same size, D = 50 µm, except for UHMWPE which was D = 20 µm. They were, however, very different in shape. Some particles, like PS, were quite spherical, while many others like PU which were formed through cryo-milling were more disk like. The primary effect of particle shape was to change the flowability of the particles from the hopper. Spherical particles were found to flow from the hopper much more easily and resulted in a uniform flux of particles from the hopper. Flatter and more faceted particles tended to flow from the hopper less smoothly resulting in intermittent spray under some deposition conditions and requiring processing at temperatures farther from their glass transition temperature. Cold spray deposition of the powder particles were studied on sheets of low-density polyethylene (LDPE) (McMaster-Carr) with a melt temperature of T_m = 110 °C and a glass transition temperature of T_g = − 90 °C. Results for cold spray deposition on an array of other polymeric and inorganic substrates can be found in our previous publications (Ref 3, 4).

A laboratory-scale cold spray system using a consumer grade single-stage air compressor with the capability of accelerating particles up to Mach 2 was used to deposit the polymeric particles. A full description of the system used in these experiments can be found in Bush et al. (Ref 3). In this system, the high-pressure gas traveled through filters and a pressure regulator before entering a heated pressure vessel which housed the powder feeder. The hot gas/powder mixture then exited the vessel and passed through the nozzle. The powder and process gas were heated together and mixed well upstream of the nozzle. The nozzle used in this study had an inlet, throat, and exit diameter of 9.5, 1.6, and 1.9 mm, respectively. The converging section measured 3 cm long, while the diverging section was 0.3 cm long and fed a 4.2 cm long constant-area extension section which was added to maximize particle residence time and exit velocity. The aluminum pressure vessel was heated with three 500 W band heaters (Omega MB-1). The temperature of the pressure vessel was monitored with an internal bore thermocouple (Omega BT) inserted through a radial pressure fitting near the bottom of the barrel and was controlled with a PID temperature controller (Omega CN2110). Nozzle inlet conditions were monitored via a thermocouple and a pressure transducer (Omega PX309-300GV) inserted just upstream of the nozzle. Powder feed was accomplished by routing the carrier air around a vibratory powder dispenser contained in the pressure vessel. A pneumatic vibrator (Cleveland Vibrators VM-25) was mounted on a connecting rod above the pressure vessel. The connecting rod ran through a slip-fit bushing and into the vessel, where it transmitted

Table 1 Physical and mechanical properties of the feedstock particles

Materials	T_g, °C	T_m, °C	D, µm	Yield strength, MPa	Density, kg/m^3	Molecular weight, kg/mol	Source
HDPE	− 90	128	48 ± 18	20	990	180	BYK Ceraflour
Polyurethane	− 63	92	50 ± 11	24	985	…	KU Leuven
Polyamide 12	97	180	50 ± 25	50	1010	…	EOS
Polystyrene	100	175	44 ± 4	34	1040	250	Microbeads
UHMWPE	− 150	130	20 ± 7	22	949	3000	Mipelon™

vibration to an attached aluminum tube that contained the powder to be deposited. The bottom of the tube was capped with coarse wire mesh, which allowed agitated powder to fall into the surrounding carrier gas.

A temperature-controlled two-dimensional (2D) *xy*-stage operated by an open source software package designed for three-dimensional (3D) printing (Repetier-Host) was used to move the substrate underneath the nozzle exit at controlled speeds to create deposition patterns consisting of one-dimensional (1D) lines and 2D square patterns. The stage could maintain a temperature of up to $T = 100$ °C during deposition. Here, all 2D deposition patterns were 2 cm × 2 cm squares. These patterns required multiple passes to deposit and used 25% overlap between sequential lines to produce a uniform and flat pattern. The overlap percentage was optimized for specific conditions of particle size, velocity, and flowrate. Specifically, $D = 50$ μm particles traveling at $V_i = 150$ m/s and with a powder feed rate of $\dot{m}_p = 35$ g/min.

A 1D inviscid model of gas and particle dynamics created by Champagne et al. was used to calculate the velocity, temperature, and pressure variations through the nozzle (Ref 36-38). This model assumes that the particles do not disturb the flow field but are acted on by the surrounding gas with drag coefficient based on their size and gas velocity and a heat transfer coefficient based on their velocity. The velocity and temperature evolution for the both the polymer particles and the glass beads were calculated as a function of position along the converging–diverging Laval nozzle to determine the impact temperature and velocity of each polymer powder. For simplicity, the powders and beads were assumed to be spherical which is clearly not always the case and the temperature was assumed to be uniform across their cross section or that they are lumped. Both assumptions and the errors they introduce are discussed in detail in Bush et al. (Ref 3).

Windows of deposition were developed over the temperature–velocity space for polymer particles with and without the additive glass beads. Particle temperature varied from room temperature to roughly 80% of T_m of the studied polymer particle, and particle velocity was studied over 75-400 m/s range. The size of the additive glass beads varied between 20 and 120 μm and were added in different amounts. The glass beads were initially mechanically mixed with the feedstock and then further mixed using an ultrasonic mixer for 30 min to ensure that all aggregates were broken down.

Imaging of both coating surface and cross section was performed on a FEI Magellan 400 XHR-SEM with nanometer resolution operated at 13 kV. To ensure accurate void identification, three images were taken at slightly different angles and then were compared with each other. A thin gold coating was applied before SEM observation by ion sputtering.

An atomic force microscopy (AFM) (Asylum, Cypher ES with an ANSCM-Pt-200 tip) was used to measure the surface roughness of the cold spray depositions. The AFM was operated at a frequency between 43 and 81 kHz using a scan rate of 1.59 Hz, a maximum scan range of 30 μm × 30 μm, and a spring constant of 1-5 N/m. The sample was placed horizontally on the object stage; the desired area was selected using an optical microscope equipped on the AFM instrument. Multiple locations were probed on each sample surface in order to probe a 2 cm^2 interrogation area, and the surface information was averaged over all the scans to obtain surface roughness statistics.

Results and Discussion

Effect of the Concentration of Glass Peening Particles on Deposition Efficiency

In the first set of experiments presented here, the effect that the addition of glass bead peening particles has on the deposition efficiency of a number of different polymer powders including HDPE, PU, PA, PS and UHMWPE was investigated. The initial studies focus on the effect of glass bead size, concentration, and impact velocity. The cold spray deposition efficiency of HDPE particles on an LDPE substrate is presented in Fig. 1 as a function of the percentage of the added glass beads under different spray conditions. The glass beads were mechanically mixed into the polymer powders and were well dispersed before being loaded into the hopper. The glass beads and the HDPE particle had diameters of $D = 40 \pm 15$ μm and $D = 48 \pm 18$ μm, respectively. A set of microscopy images of the glass beads are presented in Fig. 2. The variation in the diameter resulted in some uncertainty in the calculated particle velocities and temperatures presented in the results that follow. Separation of the glass beads from the polymer powders due either to the density or size differences of the particles was not observed during storage or in the hopper during the cold spray process.

For all the particle velocities studied, the addition of a low concentration of glass peening particles to the HDPE powder was found to increase the cold spray deposition efficiency above that of pure HDPE powders. For the subsonic cold spray conditions presented in Fig. 1a, adding 10 wt.% glass beads to the HDPE powder was found to increase the deposition efficiency from 7.7 to 10%. This 43% improvement in the deposition efficiency is well outside the error bars in the data and can therefore be considered significant. It can therefore be concluded that

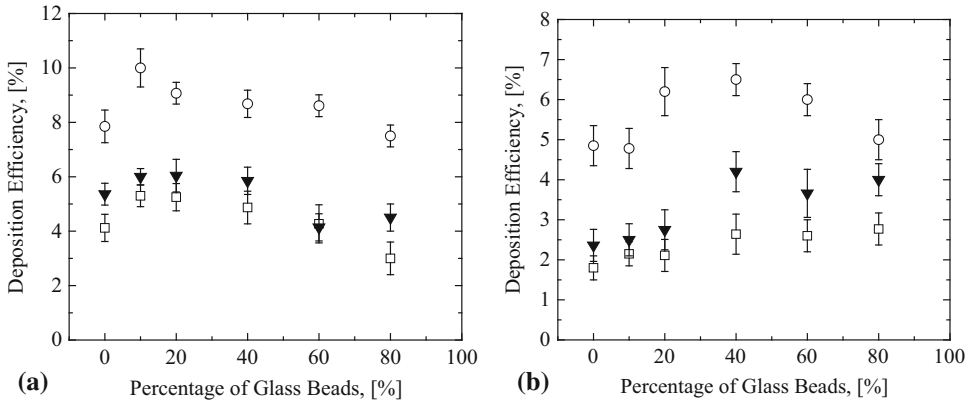

Fig. 1 Cold spray deposition efficiency of HDPE on an LDPE substrate as a function of the weight percentage of glass beads added. Data include data from both (a) a subsonic nozzle with V_{HDPE} = 275 ± 15 m/s and $V_{glass\ beads}$ = 265 ± 15 m/s, and (b) a supersonic nozzle with V_{HDPE} = 375 ± 20 m/s and $V_{glass\ beads}$ = 360 ± 20 m/s. The data include results for cold spray conditions (open square) $T_p = T_s$ = 20 °C, (filled inverted triangle) T_p = 80 °C and T_s = 20 °C, and (open circle) T_p = 80 °C and T_s = 100 °C

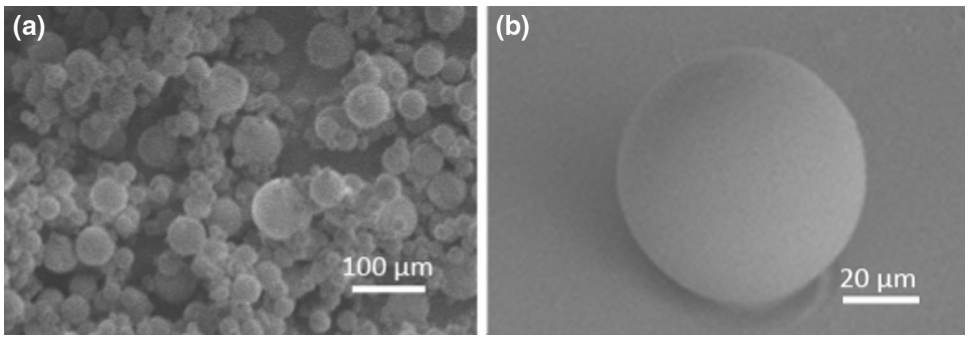

Fig. 2 SEM images of (a) an assortment of glass beads showing their morphology and the variation in size and (b) a single glass bead to highly its spherical shape

the addition of a modest amount of glass beads as peening particles can greatly improve the deposition efficiency of polymer powders. However, there appears to be an optimal amount of peening particle addition. Increasing the glass bead concentration beyond 10% in the case of subsonic particle speeds, as shown in Fig. 1a, and beyond 40% in the case of supersonic speeds, as shown in Fig. 1b, was found to result in a decrease in deposition efficiency, although it should be noted that the deposition efficiency with less than 60 wt.% glass peening particles was found to be as high or higher than the pure HDPE powder in both cases. Similar improvements were observed for processing conditions with the particles and substrate held at different temperatures including room temperature. It should be noted here that SEM images of the HDPE coatings revealed no deposition of glass particles for any of the subsonic experiments presented in Fig. 1a. However, for the case of supersonic experiments presented in Fig. 1b, a small fraction of glass beads (less than 5%) was deposited. As the deposition efficiency is calculated by weighting the LDPE substrate before and after the spray process and comparing the increase in weight to the weight of polymer sprayed, the adhesion of glass particles can affect the results of the deposition efficiency reported in Fig. 1b. To correct errors due to glass bead adhesion, the approximate weight of the deposited glass beads was subtracted from the final weight of the substrate before calculating the deposition efficiency. Similar trends with weight percent of glass beads were observed for all polymers studied.

Effect of the Size of Glass Peening Particles on Deposition Efficiency

In order to study the effect of the size of the glass bead peening particles, 10 wt.% of four different diameter glass beads of 20 ± 10, 40 ± 15, 70 ± 25, and 120 ± 25 µm was added to the HDPE, UHMWPE, PU, PA, and PS polymer powders. The deposition efficiency is plotted in Fig. 3 for each of the four different sizes of glass beads paired with each polymer powder. The processing conditions in each case were held fixed such that the polymer powder temperature was maintained at T_p = 80 °C, the LDPE substrate was held at T_s = 100 °C, and the pressure drop was set such that the polymer particle velocity was consistent at V_p = 275 m/s. It is important to note, however, that the impact velocity of the glass beads was not constant across the experiments, because the acceleration of the glass beads through the Laval nozzle is a function of

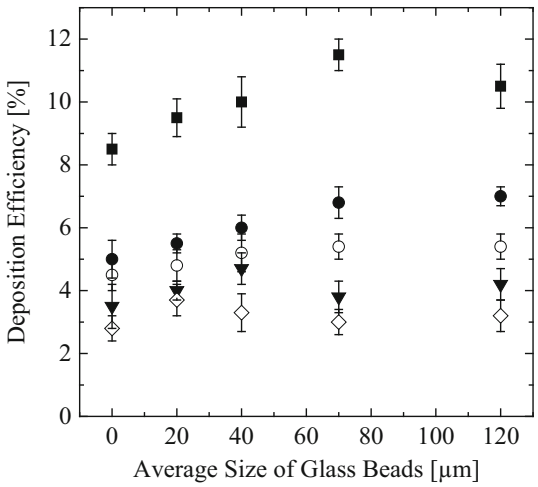

Fig. 3 Cold spray deposition efficiency as a function of the average size of the glass beads added as peening particles. In all cases, 10 wt.% of glass beads were added to (filled square) HDPE, (filled circle) PU, (open circle) PA, (filled inverted triangle) PS, (open diamond) UHMWPE. The substrate was LDPE, the particle temperature was T_p = 80 °C, substrate temperature was T_s = 100 °C, and the polymer particle velocity was 275 ± 15 m/s

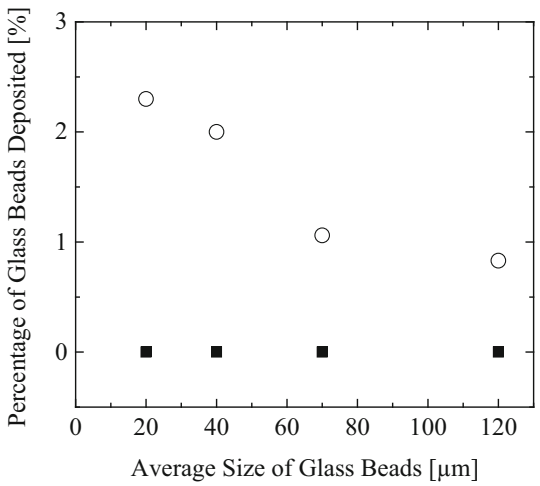

Fig. 4 (a) Deposition percentage of the glass beads cold-sprayed on an LDPE substrate at room temperature using both a (filled square) subsonic nozzle, and a (open circle) supersonic nozzle, the glass beads velocity ranges between 100 and 260 m/s in the subsonic condition and between 340 and 370 m/s in the supersonic conditions, both particle and substrate are at room temperature, $T_p = T_s$ = 20 °C

the diameter of the bead. As a result, the impact velocity of the glass beads was calculated to decrease from 310 to 245 m/s as the size of the glass beads increased from 20 to 120 μm. Over the same increase in diameter, the kinetic energy of each particle upon impact with the substrate increased by a factor of nearly 135. However, because all the experiments were performed with the same weight fraction of glass beads added to the polymer powder increasing the glass bead diameter from 20 to 120 μm resulted in 216 times fewer particles in the polymer powder, the same number of fewer peening impacts and a 37% reduction in the overall kinetic energy available for peening the substrate.

As shown in Fig. 3, all of the polymer powders showed a slight increase in the deposition efficiency with increasing glass bead diameter. The largest effects were observed for the HDPE particles for which an increase in deposition efficiency from DE = 8% to 11% was observed. The increase in deposition efficiency with increasing peening particle size is likely the result of the increased kinetic energy of the individual glass particle. However, as seen for each polymer, an optimal size for the glass beads exists beyond which the deposition efficiency was found to plateau or even decrease. This decrease at larger glass bead diameters might be a result of the reduction in the number of peening particle impacts or it might suggest that there is an upper limit in the kinetic energy of the peening particles beyond which surface ablation begins. Interestingly, the optimal glass bead size was found to be roughly the size of the polymer powder in each case. Given the density of the glass particle and the velocity obtained during flight that size corresponds to an impact kinetic energy that is roughly four times the impact kinetic energy of the polymer powders.

Deposition of Glass Beads on an LDPE Substrate

In analyzing the effect of glass beads on the deposition efficiency, it is necessary to confirm that the glass beads are in fact non-adhesive and are not depositing with the polymer powder on the substrate surface. This unwanted deposition would change the composition and properties of the deposited film and could negatively affect the outcome of the cold spray deposition. In order to ensure that the glass beads did not adhere to the surface, batches of 100% glass beads were directly cold-sprayed at the processing conditions used above on an LDPE substrate. In Fig. 4, the deposition percentage of the glass beads is plotted against the glass bead average size after accelerating the pure glass beads to the subsonic velocity range of V_i = 245–310 m/s and the supersonic velocity range of V_i = 340–370 m/s. The glass beads did not adhere to the LDPE substrate when traveling below the speed of sound, Ma < 1. However, above Ma > 1, some glass beads did in fact deposit on the LDPE substrate. The deposition percentage of the glass beads was found to decrease from 2.25 to 1% as the average glass bead size increased from 20 to 120 μm. The speed of the glass beads calculated using the 1D inviscid model of gas and particle dynamics (Ref 38) predicts a linear decrease in velocity from 370 to 340 m/s as the glass bead size increased from 20 to 120 μm in the supersonic

flow conditions in Fig. 4 which might account for the reduced percentage of deposition of the glass beads.

Microstructural Studies of Deposited Polymer Films

Evidence for glass bead adhesion can also be seen in the SEM images of cold spray depositions of HDPE and other polymers mixed with glass beads when they are processed at supersonic velocities. An SEM image of a cold spray deposition of HDPE particles with the addition of 10 wt.% glass beads on an LDPE substrate is presented in Fig. 5. The presence of glass beads is clearly evident in Fig. 5. The glass beads have been deposited and incorporated into the HDPE layer deposited on the LDPE substrate. SEM image of top view and cross-sectional view of the cold-sprayed HDPE and PU particles on an LDPE substrate under subsonic conditions are presented in Fig. 6. In contrast to the case for supersonic particle impact in Fig. 5, no traces of the glass beads are visible in either the top views or the cross-sectional views of the cold-sprayed HDPE and PU deposited layer in Fig. 6. A smooth and dense deposition is visible in the top views in Fig. 6(a) and (c) showing little porosity and a mixed and homogeneous interface between the deposited layer of HDPE and PU and the LDPE substrate can be seen in the cross-sectional views in Fig. 6(b) and (d). Similar results were observed in SEM studies of PA, PS, and UHMWPE deposited layers.

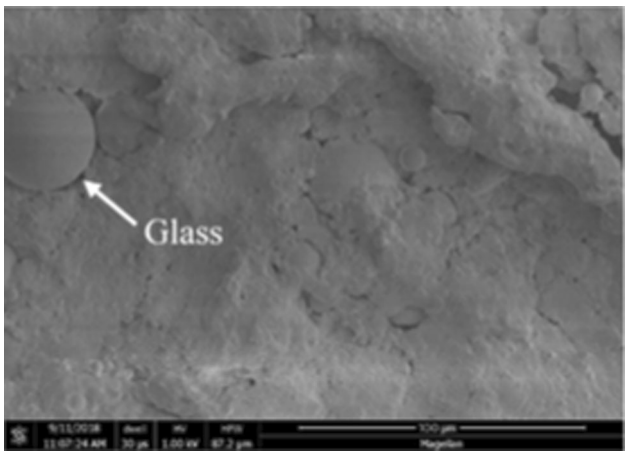

Fig. 5 SEM images of cold spray deposition of HDPE particles with the addition of 10 wt.% glass beads on an LDPE substrate using supersonic processing condition with a particle impact velocity of V_i = 370 m/s. The glass beads used in this experiment had a diameter of $D = 20 \pm 10$ μm and can be seen in the upper left of the image, deposited in the HDPE matrix

Effect of the Addition of Glass Peening Particles on Deposition Window

In addition to increasing the deposition efficiency of polymer powders, the secondary goal of adding peening particles was to expand the deposition window for polymer powders, especially hard-to-deposit polymers like UHMWPE. The effect of adding glass beads to the polymer particles on the deposition window is shown in Fig. 7 for all of the polymer powders studied here. The trend line for the transition from unsuccessful to successful deposition for the pure polymer powders was taken from the literature (Ref 3, 35) and has been superimposed over the data in Fig. 7 to highlight the effect of the addition of the glass beads. It can be seen from this figure that the deposition window has been expanded by the addition of peening particles. Excluding UHMWPE, in all cases, the minimum particle impact velocities needed for deposition was shifted to lower velocities over all the particle temperatures studied here. For example, as seen in Fig. 7(a), for the HDPE particles the critical impact velocity was found to decrease from 100 to 75 m/s at room temperature and from 80 to 65 m/s at the particle temperature of T_p = 80 °C. The slopes of the variation of the lower critical impact velocity with temperature in Fig. 7(a)-(d) show little variation between the case of cold-sprayed pure polymer powders and the case of cold-sprayed polymer powders with 10 wt.% glass beads. Similar effects were observed in extension of the deposition map to lower impact velocities for the PU and PA particles shown in Fig. 7(b) and (d).

The cold spray results for PS powders shown in Fig. 7(c) show a modest reduction of 5 to 10 m/s in the minimum impact velocity for successful deposition after the addition of 10 wt.% of the glass beads. However, unlike the HDPE data presented in Fig. 7(a), the PS data also contain an upper velocity limit beyond which deposition was not possible due to ablation of poorly adhered particles. From Fig. 7(c), it is clear that the addition of peening particles can also improve the window of deposition by increasing the maximum impact velocity for successful deposition when it exists. For the case of PS, the maximum impact velocity was shifted upwards by 15 m/s resulting in a broadening of the deposition window on both ends.

Finally, as seen in Fig. 7(e), of all the powders tested, the UHMWPE presents the most stark contrast in the deposition window before and after the addition of glass peening particles. Without the addition of glass beads, the deposition of UHMWPE below T_p = 60 °C was not possible. Amazingly, after the addition of 10 wt.% glass beads to the UHMWPE powder, deposition was achieved at room temperature at subsonic velocities and with efficiencies of nearly 3%. That the deposition occurred at subsonic

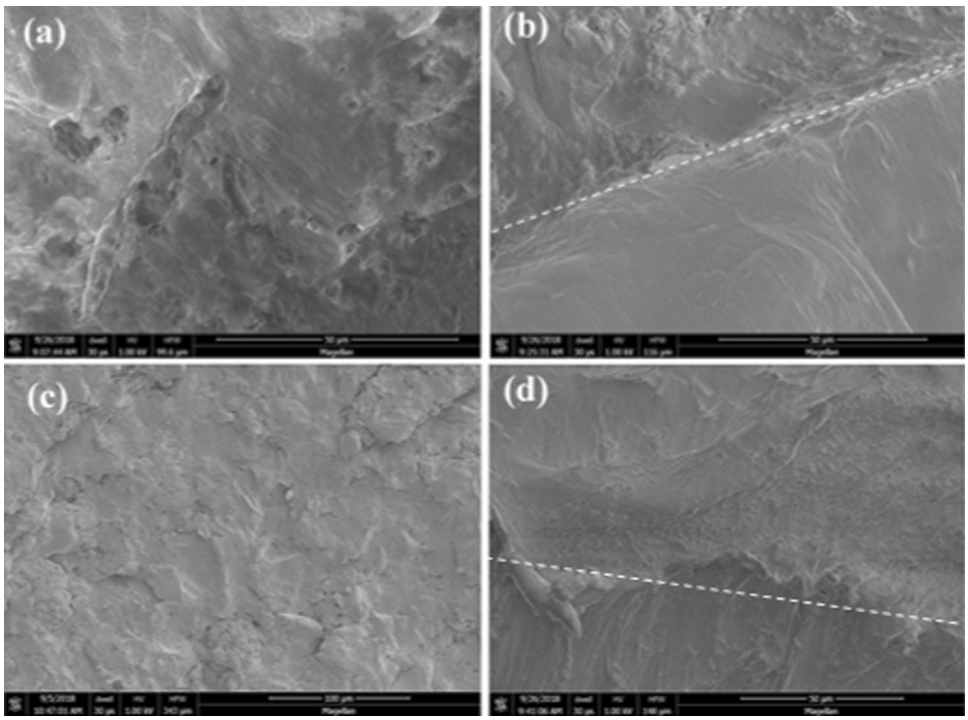

Fig. 6 SEM images of (a) the top view and (b) the cross-sectional view of HDPE particles along with (c) the top view and (d) the cross-sectional view of PU particles deposited on an LDPE substrate. Experiments were performed at particle temperature of T_p = 60 °C, substrate temperature of T_s = 100 °C, and particle impact velocity of V_i = 270 m/s with 10 wt.% glass beads added to the polymer powders

velocities is important, as it means that deposition was viable over a range of velocities where glass beads will not become incorporated into the final UHMWPE coating. Interestingly, unlike all of the other polymers tested, the deposition windows of UHMWPE in Fig. 7(e) were not significantly expanded to lower impact velocities with the addition of the 10 wt.% glass beads to the UHMWPE powder.

Effect of the Glass Peening Particles on Surface Roughness

Using atomic force microscopy, the surface roughness of the deposited polymer films were studied for all the polymer powders studied with and without the addition of glass peening particles. AFM was chosen for its superior spatial resolution. A number of AFM test windows were stitched together to interrogate a 2 cm^2 area of the cold spray deposited polymer film. Figure 8 shows the results for HDPE which are representational of the result for all the polymer powders tested. The surface roughness of a melt-cast HDPE surface was found to be L = 0.6 μm. Cold spray deposition on either LDPE or a melt-cast HDPE surface had little effect on the final surface roughness of the deposited layer. In both cases, the cold spray deposition of a pure HDPE powder resulted in a surface roughness of L = 1.2 μm. This surface roughness is twice as large as the melt-cast HDPE surface, but far smaller than the size of an individual HDPE powder particle which is roughly 40 μm. Evidence of individual particles is not clearly present in the AFM measurements or the microscopy images shown previously in Fig. 6. After the addition of 10 wt.% glass beads to the HDPE powder, the surface roughness of the cold spray deposition was reduced to L = 0.5 μm. This observation suggests that the use of peening particles in polymer cold spray can help reduce the final surface roughness of the deposited film. In the case of HDPE, the addition of peening particles improved the surface roughness of the cold spray deposition to the point where it was comparable to the melt-cast surface. Similar results were also observed for all the other polymer powders tested.

These results have positive implications for the final finish of the cold spray deposited layer, but they also help explain the increased deposition efficiency observed after the addition of peening particles. Our previous work suggested that deposition occurred for polymer powders only below a critical particle–substrate impact angle (Ref 35). Surface roughness can cause failure of particle deposition if the impact is at too acute an angle to the local roughness. In addition, single particle impact measurements show modest plastic deformation of successfully deposited particles (less than 10% for high T_g particles and less than 50% for low T_g particles (Ref 4) meaning that they can be easily sheared off by secondary particles, but also cause a dramatic increase in the surface roughness. Peening particles clearly help smooth the overall surface and flatten

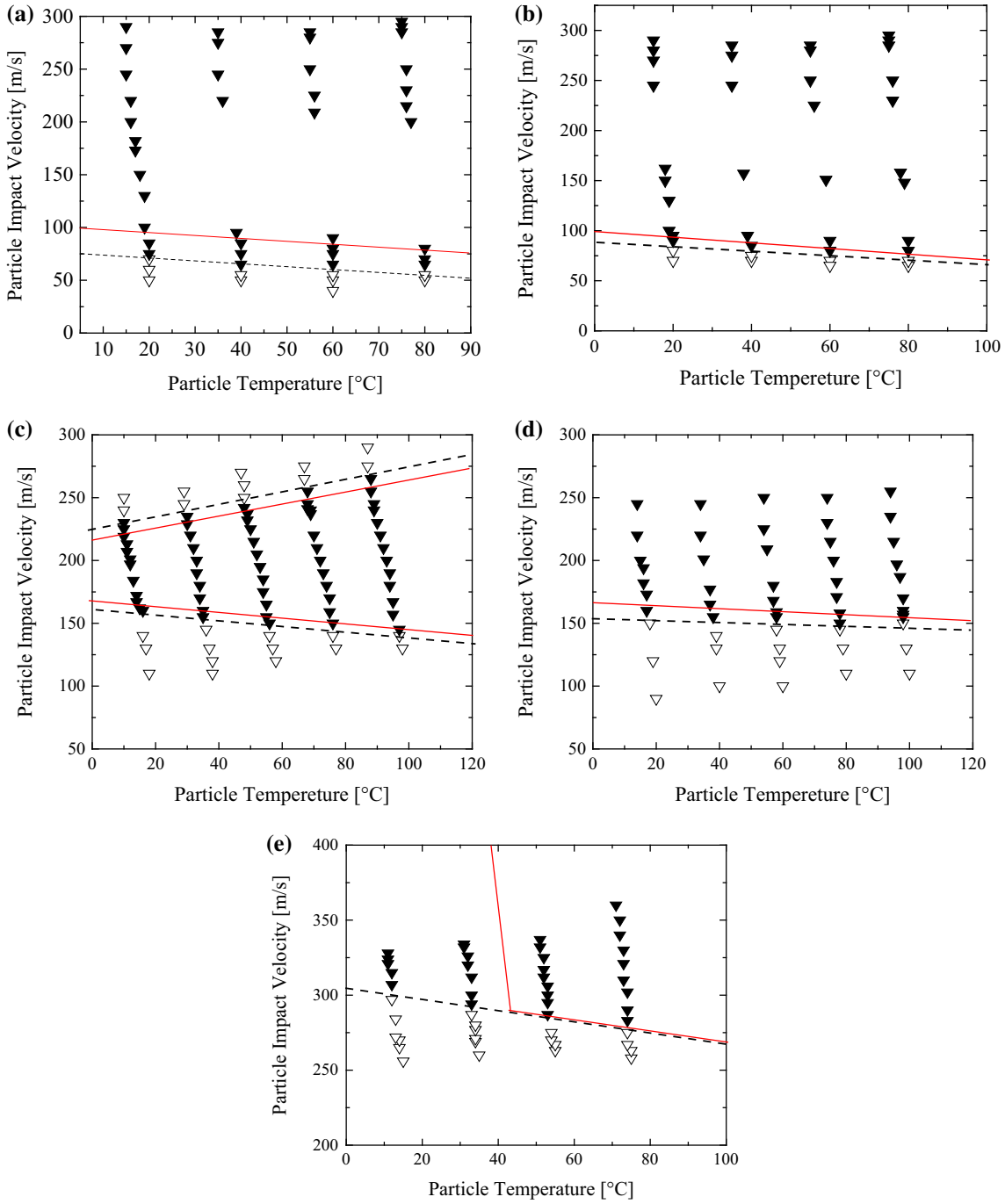

Fig. 7 Cold spray deposition window for (a) HDPE, (b) PU, (c) PS, (d) PA, and (e) UHMWPE particles with the addition of 10 wt.% of glass beads. The LDPE substrate temperature was fixed at T_s = 100 °C in all experiments. The data include (filled inverted triangle) successful deposition, (open inverted triangle) unsuccessful deposition and lines showing the approximate transition from unsuccessful to successful deposition for the polymer powder (dashed line) with and (solid line) without the addition of glass peening particles

already deposited particles making them more strongly adhered and more conducive for successful deposition of the successive polymer particle during impact. As another evidence to show the important role of the surface roughness in deposition, the deposition efficiency on the smooth surface was measured to be 22% larger than on the rough surfaces for HDPE particles depositing on a smooth HDPE surface and a roughened HDPE surface with a

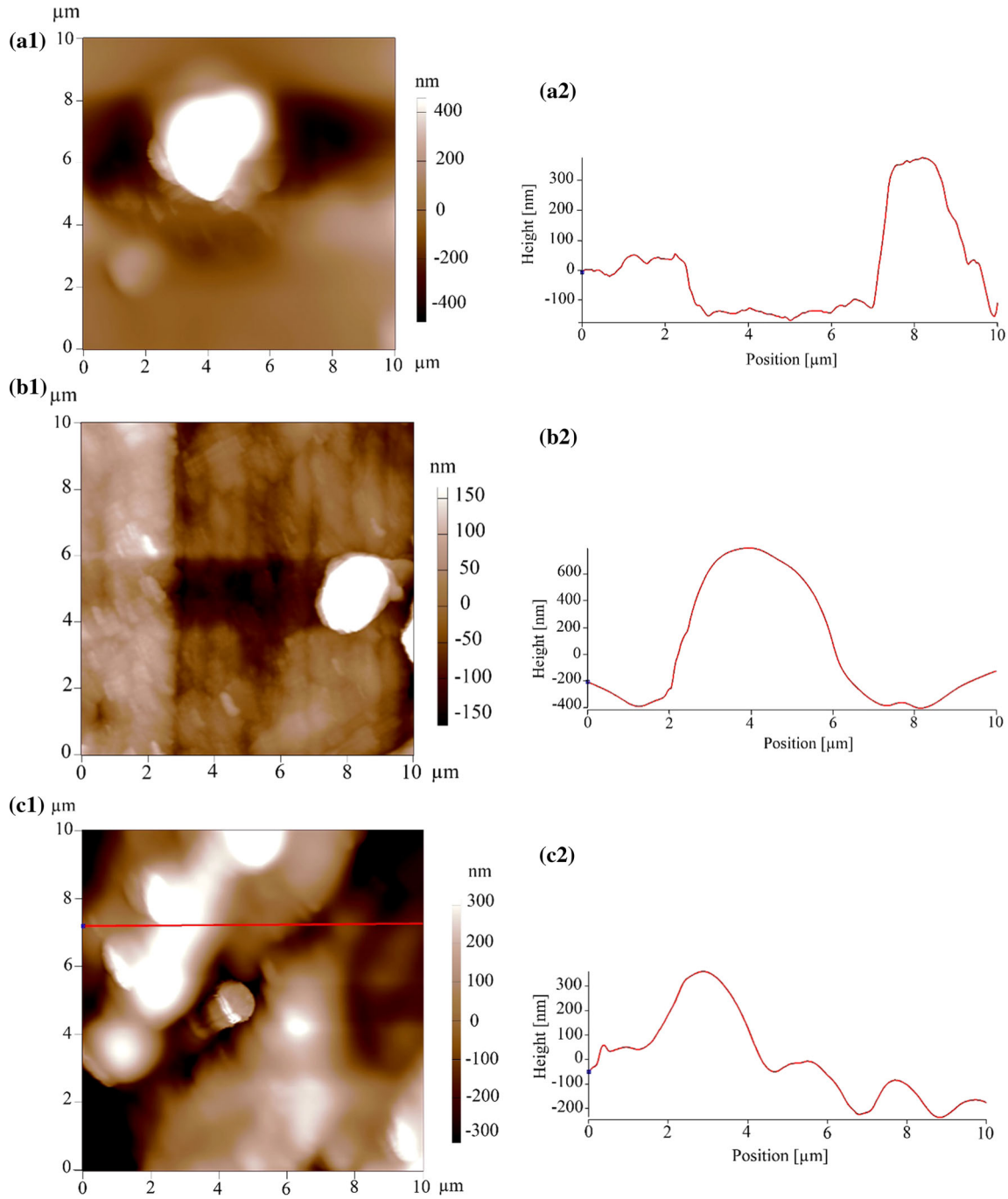

Fig. 8 2D AFM images of (a1) a melt-cast HDPE substrate, (b1) a cold-sprayed HDPE sample on an LDPE substrate, and (c1) a cold-sprayed HDPE deposition with 10 wt.% added glass beads, and (a2), (b2), c2) the section analysis of 2D images. The particle temperature, substrate temperature, and particle impact velocity were T_p = 60 °C and T_s = 100 °C and V_i= 275 m/s in the cold spray process—provided by Z. Zhu

120-grit sandpaper. This is consistent with our observation in using the peening particles where deposition efficiency was improved by 28–37% for the studied polymers after adding 10% glass beads to the particle batch as can be seen in Fig. 3.

Conclusions

Glass beads of a wide variety of different sizes were systematically added to batches of HDPE, PU, PA, PS, and UHMWPE cold spray powders to study of peening particles on the cold spray deposition of polymers. The addition of 10 wt.% sacrificial non-adhesive glass beads to the polymer particles was found to expand the deposition windows of all the polymer powders tested. For polymers powders like HDPE, for which only a minimum and no maximum critical impact velocity was observed, the addition of peening particles was found to decrease the minimum impact velocities needed for successfully deposition by 25-30 m/s at a given polymer and substrate temperature. For polymers powders like PS, which showed an both a minimum and maximum critical impact velocity, the addition of peening particle was found to both decrease the minimum impact velocity and increase the maximum impact velocity for which successful deposition was possible by 10-15 m/s. For polymer powders like UHMWPE, which showed a critical particle temperature of T_p = 60 °C below which deposition was not possible, the addition of peening particle was found to extend the deposition window all the way to room temperature, T_p = 20 °C. From these experiments, it can be concluded that the addition of peening particles can significantly widen the cold spray window of deposition accessible for polymer powders.

The addition of glass peening particle was also shown to significantly increase the cold spray deposition efficiency of polymer powders. The deposition efficiency was measured as a function of the size and concentration of the glass beads. The deposition efficiency was found to increase with increasing glass peening particle size before reaching a maximum that roughly coincided with the size of the polymer powder. For subsonic cold spray deposition, the deposition efficiency was found to increase quickly with particle concentration before reaching a maximum at roughly 10 wt.% of glass peening particles. Across all the polymer powders tested, the addition of peening particles was found to increase the cold spray deposition efficiency by as much as 30–40% from the case of the pure polymer powder. Thus, the addition of peening particles can significantly improve the deposition efficiency of polymer cold spray.

The increase in deposition efficiency and the expansion of the deposition window is the result of the additional plastic deformation and energy dissipation in the substrate induced by the head-on collisions of the dense, high-energy peening particles. The peening particles were found to flatten the deposited polymer particles resulting in a smoother and more uniform deposition layer. As long as the deposition was performed with subsonic particle velocities, the microstructural SEM studies revealed no deposition of glass peening particles in either the LDPE substrate or the final cold spray deposited film. Thus, the addition of peening particles appears to be a valuable tool for improving the efficiency of the cold spray process for polymer powders and the quality of the final deposited polymer films.

Acknowledgments This research was accomplished through a cooperative research agreement with the US Army Research Laboratory, Contract: W911NF-15-2-0024, P00003 'Intelligent Processing of Materials by Design.' The authors would also like to thank Peter van Puyvelde of KU Leuven for kindly supplying us with the PS, PA, and PU powders used in this study. The contributions from Zimu Zhu who provided the AFM studies are also appreciated.

Appendix

Figure 9 shows the optical microscopy of deposition of HDPE particles (a) on HDPE substrate with smooth surface and (b) on a roughened HDPE surface. The experiment of depositing HDPE particles on a smooth and a roughened surface of HDPE showed that the deposition efficiency was improved by 22% when depositing on a smooth surface compared to depositing on a rough surface of HDPE

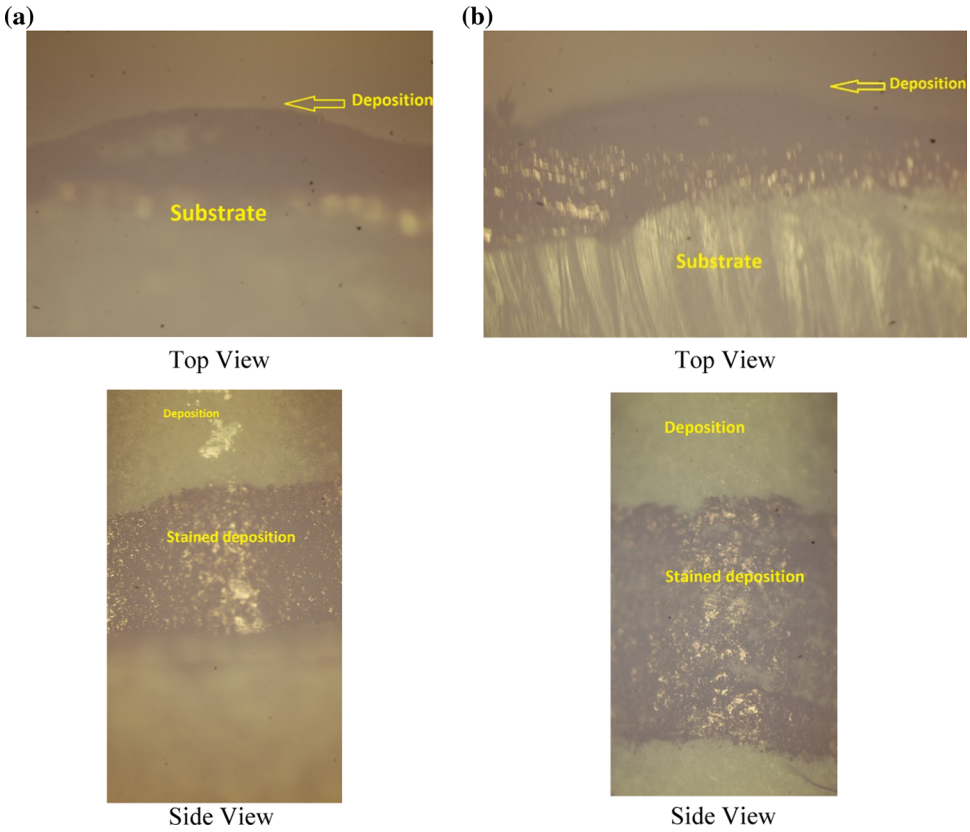

Fig. 9 Optical microscopy of deposition of HDPE particles (a) on HDPE substrate with smooth surface and (b) on a roughened HDPE surface

substrate. This information is not visible the optical images. Rather, the measurement was done by weighing the substrate before an after deposition to calculate the deposition efficiency. Therefore, as a response to the reviewer's comment, we provided these images in the Appendix not in the results and discussion section.

References

1. F.S. da Silva, N. Cinca, S. Dosta, I.G. Cano, J.M. Guilemany, C.S.A. Caires, A.R. Lima, C.M. Silva, S.L. Oliveira, A.R.L. Caires, and A.V. Benedetti, Corrosion Resistance and Antibacterial Properties of Copper Coating Deposited by Cold Gas Spray, *Surf. Coat. Technol.*, 2019, **361**, p 292-301
2. A. Papyrin, V. Kosarev, S. Klinkov, A. Alkhimov, and V.M. Fomin, *Cold Spray Technology*, Elsevier, Amsterdam, 2007
3. T.P. Bush, Z. Khalkhali, V.K. Champagne, D.P. Schmidt, and J.P. Rothstein, Optimization of Cold Spray Deposition of High-Density Polyethylene Powders, *Therm. Spray Technol.*, 2017, **26**(7), p 1548-1564
4. Z. Khalkhali, W. Xie, V.K. Champagneb, J.-H. Lee, and J.P. Rothstein, A Comparison of Cold Spray Technique to Single Particle Micro-ballistic Impacts for the Deposition of Polymer Particles on Polymer Substrates, *Surf. Coat. Technol.*, 2018, **351**, p 99-107
5. A. Astarita, L. Boccarusso, M. Durante, A. Viscusi, R. Sansone, and L. Carrino, Study of the Production of a Metallic Coating on Natural Fiber Composite Through the Cold Spray Technique, *Mater. Eng. Perform.*, 2018, **27**(2), p 739-750
6. G. Archambault, B. Jodoin, S. Gaydos, and M. Yandouzi, Metallization of Carbon Fiber Reinforced Polymer Composite by Cold Spray and Lay-Up Molding Processes, *Surf. Coat. Technol.*, 2016, **300**, p 78-86
7. H. Assadi, T. Schmidt, H. Richter, J.-O. Kliemann, K. Binder, F. Gartner, T. Klassen, and H. Kreye, On parameter Selection in Cold Spraying, *J. Therm. Spray Technol.*, 2011, **20**(6), p 1161-1176
8. M. Gardon, A. Latorre, M. Torrell, S. Dosta, J. Fernandez, and J.M. Guilemany, Cold Gas Spray Titanium Coatings Onto a Biocompatible Polymer, *Mater. Lett.*, 2013, **106**, p 97-99
9. A.M. Vilardell, N. Cinca, A. Concustell, S. Dosta, I.G. Cano, and J.M. Guilemany, Cold Spray as an Emerging Technology for Biocompatible and Antibacterial Coatings: State of Art, *Mater. Sci.*, 2015, **50**, p 4441-4462
10. X. Zhou and P. Mohanty, Electrochemical Behavior of Cold Sprayed Hydroxyapatite/Titanium Composite in Hanks' Solution, *Electrochim. Acta*, 2012, **65**, p 134-140
11. N. Cinca, A.M. Vilardell, S. Dosta, A. Concustell, I. Garcia Cano, J.M. Guilemany, S. Estrade, A. Ruiz, and F. Peiro, A New Alternative for Obtaining Nanocrystalline Bioactive Coatings: Study of Hydroxyapatite Deposition Mechanisms by Cold Gas Spraying, *Am. Ceram. Soc.*, 2016, **99**, p 1420-1428
12. M. Robotti, S. Dosta, C. Fernandez-Rodriguez, M.J. Hernandez-Rodriguez, I.G. Cano, E.P. Melian, and J.M. Guilemany, Photocatalytic Abatement of NO_x by $CTiO_2$/Polymer Composite Coatings Obtained by Low Pressure Cold Gas Spraying, *Appl. Surf. Sci.*, 2016, **362**, p 274-280
13. L. Wang, F. Wang, S. Li, and Y. Wang, Microstructure and Application of Alumina-Supported Cu-Based Coating Prepared by Cold Spray, *Surf. Coat. Technol.*, 2019, **362**, p 113-123

14. M.J. Vucko, P.C. King, A.J. Poole, Y. Hu, M.Z. Jahedi, and R. de Nys, Assessing the Antifouling Properties of Cold-Spray Metal Embedment Using Loading Density Gradients of Metal Particles, *Biofouling*, 2014, **30**, p 651-666
15. C. Stenson, K.A. McDonnell, S. Yin, B. Aldwell, M. Meyer, D.P. Dowling, and R. Lupoi, Cold Spray Deposition to Prevent Fouling of Polymer Surfaces, *Surf. Eng.*, 2018, **34**(3), p 1-11
16. H. Che, P. Vo, and S. Yue, Investigation of Cold Spray on Polymers by Single Particle ImpactExperiments, *Therm. Spray Technol.*, 2019, **28**, p 135-143
17. P.A. Podrabinnik and I.V. Shishkovsky, Laser Post Annealing of Cold-Sprayed Al-Ni Composite Coatings for Green Energy Tasks, *Procedia IUTAM*, 2017, **23**, p 108-113
18. F. Robitaille, M. Yandouzi, S. Hind, and B. Jodoin, Metallic Coating of Aerospace Carbon/Epoxy Composites by the Pulsed Gas Dynamic Spraying Process, *Surf. Coat. Technol.*, 2009, **203**(19), p 2954-2960
19. H. Che, M. Gagne, P.S.M. Rajesh, J.E. Sapieha, F. Sirois, D. Therriault, and S. Yue, Metallization of Carbon Fibre Reinforced Polymer for Lightning Strike Protection, *Mater. Eng. Perform.*, 2018, **27**(10), p 5205-5211
20. H. Che, P. Vo, and S. Yue, Metallization of Carbon Fibre Reinforced Polymers by Cold Spray, *Surf. Coat. Technol.*, 2017, **313**, p 236-247
21. H. Che, X. Chu, P. Vo, and S. Yue, Cold Spray of Mixed Metal Powders on Carbon Fibre Reinforced Polymers, *Surf. Coat. Technol.*, 2017, **329**, p 232-243
22. J. Affi, H. Okazaki, M. Yamada, and M. Fukumoto, Fabrication of Aluminum Coating onto CFRP Substrate by Cold Spray, *Mater. Trans.*, 2011, **52**(9), p 1759-1763
23. P.S.M. Rajesh, F. Sirois, and D. Therriault, Damage Response of Composites Coated with Conducting Materials Subjected to Emulated Lightning Strikes, *Mater. Des.*, 2018, **139**, p 45-55
24. R. Kromer, Y. Danlos, E. Aubignat, C. Verdy, and S. Costil, Coating Deposition and Adhesion Enhancements by Laser Surface Texturing—Metallic Particles on Different Classes of Substrates in Cold Spraying Process, *Mater. Manuf. Process.*, 2017, **32**(14), p 164
25. B.K. Pant, A.H.V. Pavan, R.V. Prakash, and M. Kamaraj, Effect of Laser Peening and Shot Peening on Fatigue Striations During FCGR Study of Ti6Al4 V, *Int. J. Fatigue*, 2016, **93**, p 38-50
26. G.-Q. Chen, Y. Jiao, T.-Y. Tian, X.-H. Zhang, Z.-Q. Li, and W.-L. Zhou, Effect of Wet Shot Peening on Ti-6Al-4 V Alloy Treated by Ceramic Beads, *Trans. Nonferrous Metals Soc. China*, 2014, **24**, p 690-696
27. R. Ramos, N. Ferreira, J.A.M. Ferreira, C. Capela, and A.C. Batista, Improvement in Fatigue Life of Al 7475-T7351 Alloy Specimens by Applying Ultrasonic and Microshot Peening, *Int. J. Fatigue*, 2016, **92**, p 87-95
28. H. Kovaci, Y.B. Bozkurt, A.F. Yetim, M. Aslan, and A. Celik, The Effect of Surface Plastic Deformation Produced by Shot Peening on Corrosion Behavior of a Low-Alloy Steel, *Surf. Coat. Technol.*, 2019, **360**, p 78-86
29. Q. Wu, D.-J. Xie, Z.-M. Jia, Y.-D. Zhang, and H.-Z. Zhang, Effect of Shot Peening on Surface Residual Stress Distribution of SiCp/2024Al, *Compos. B*, 2018, **154**, p 382-387
30. C. Wang, C. Jiang, F. Cai, Y. Zhao, K. Zhu, and Z. Chai, Effect of Shot Peening on the Residual Stresses and Microstructure of Tungsten Cemented Carbide, *Mater. Des.*, 2016, **95**, p 159-164
31. A. Moridi, S.M. Hassani-Gangaraj, S. Vezzu, L. Trsko, and M. Guagliano, Fatigue Behavior of Cold Spray Coatings: The Effect of Conventional and Severe Shot Peening as Pre-/Post-treatment, *Surf. Coat. Technol.*, 2015, **283**, p 247-254
32. X.-T. Luo, Y.-K. Wei, Y. Wang, and C.-J. Li, Microstructure and Mechanical Property of Ti and Ti6Al4V Prepared by an In-Situ Shot Peening Assisted Cold Spraying, *Mater. Des.*, 2015, **85**, p 527-533
33. H. Lee, H. Shin, S. Lee, and K. Ko, Effect of Gas Pressure on Al Coatings by Cold Gas Dynamic Spray, *Mater. Lett.*, 2008, **62**(10–11), p 1579-1581
34. K. Ravi, T. Deplancke, K. Ogawa, J.-Y. Cavaille, and O. Lame, Understanding Deposition Mechanism in Cold Sprayed Ultra High Molecular Weight Polyethylene Coatings on Metals by Isolated Particle Deposition Method, *Addit. Manuf.*, 2018, **21**, p 191-200
35. Z. Khalkhali and J.P. Rothstein, Characterization of the Cold Spray Deposition of a Wide Variety of Polymeric Powders, *Surf. Coat. Technol.*, 2019, **383**, p 125251
36. A.S. Alhulaifi, G.A. Buck, and W.J. Arbegast, Numerical and Experimental Investigation of Cold Spray Gas Dynamic Effects for Polymer Coating, *Therm. Spray Technol.*, 2012, **21**, p 852-862
37. A. Shapiro, *The Dynamics and Thermodynamics of Compressible Fluid Flow*, The Ronald Press Company, New York, 1953
38. V.K. Champagne, D.J. Helfritch, S.P.G. Dinavahi, and P.F. Leyman, Theoretical and Experimental Particle Velocity in Cold Spray, *Therm. Spray Technol.*, 2011, **20**, p 425-431